A Powerful Autopilot System for Small UAVs with Accurate INS/GPS Integrated Navigation

Masaru Naruoka*, Takeshi Tsuchiya**

*Department of Aeronautics and Astronautics, The University of Tokyo, Tokyo, Japan
(Tel: +81-3-5841-6568; E-mail: tt077062@mail.ecc.u-tokyo.ac.jp)
**Department of Aeronautics and Astronautics, The University of Tokyo, Tokyo, Japan
(Tel: +81-3-5841-6644; E-mail: tsuchiya@mail.ecc.u-tokyo.ac.jp)

Abstract: In this paper, a new concept for autopilot systems for small unmanned aerial vehicles (UAVs) is presented. Compared to the existing systems, the proposed system has two enhanced features: 1) accurate navigation, 2) large computational capacity. The first feature is realized by an INS/GPS (Inertial Navigation System / Global Positioning System) integrated system using small MEMS (Micro Electro Mechanical Systems) inertial sensors and a civil-use GPS receiver. This configuration is based on our previous study, and two improvements, estimation of the bias error of inertial sensors, and enhancement of the attitude observability, are performed in this study. The second feature is achieved by a DSP (Digital Signal Processor) and enables small UAVs to employ advanced guidance and control algorithms. In order to validate its functionality, a prototype system is developed, and a comparison experiment is performed with an ultra-precise navigation device, GAIA. This proves that our system provides navigation information accurate enough for controlling small UAVs.

Keywords: Autopilot, small UAV, INS/GPS, MEMS

1. INTRODUCTION

This study is motivated by today's demand for applying small UAVs, whose wing span is about one meter. Such applications include disaster monitoring, high security area monitoring, and a test bed for advanced experiments. These applications are ultimately achieved with full autonomy which is often more sophisticated than human. However, existing autopilot systems which are intended to be installed into small UAVs provide only partial autonomy. It is thought that this is maily due to lack of both the accuracy of navigation and the computational power. Therefore, a new autopilot system with two enhanced navigation and larger computational capacity, is proposed.

To enhance the navigation accuracy, a strap-down INS/GPS (Inertial Navigation System / Global Positioning System) integrated navigation system is used, because it supplies accurate and reliable navigation information. However, the strap-down INS/GPS devices which are installed in typical aircraft keep their ultra-high accuracy with big and heavy dedicated components, such as a ring laser gyro and a multi-frequency GPS receiver. In order to apply the system to small UAVs, lighter and smaller components must be used at the cost of its accuracy, because small UAVs have limitations on payload. Therefore, our previous study [1, 2], that a INS/GPS system which consists of small, light, but low accuracy MEMS inertial sensors and a civil-use GPS receiver keeps a certain level of accuracy by using "loose-coupling" Kalman filtering (KF) and quaternion algorithm, is extended to the improved autopilot presented here.

The second feature, large computational capacity, is supported with a DSP. DSPs are mostly used in the field of sound and video processing which requires instantaneous performance represented by the number of MIPS (mega instructions per second) or FLOPS (floating point operations per second). Such a DSP enables small UAVs to be controlled more intelligently through complicated modern algorithms such as inverse dynamics and H-infinity that generate heavy computational load.

In the following section, more details of the proposed system is described, and the developed prototype for validating its functionality is introduced. Section 3. highlights the improvements to our previous INS/GPS study, and a comparative experiment in real flight to measure accuracy of the navigation part of the proposed system is described in section 4.. Finally, this study is summarized in the conclusion.

2. CONCEPT AND PROTOTYPING

2.1 Concept

The proposed system has two enhanced features, and the details of which are explained in this subsection and a comparison between the proposed system and existing autopilot systems for small UAVs will be shown.

2.1.1 INS/GPS navigation

The concept of the navigation part of the existing systems is mostly that sensors and a GPS receiver provide navigation information independently. In addition, both the guidance and the control modules, which are subsequent to the navigation module, calculate commands depending on outputs which are generated by a specific component. In fact, they neither utilize all outputs, nor work correctly when the error of a component is not compensated, for example, attitude error diverges in steady rotating when the direction of the gravitational force cannot be measured because of the centrifugal force.

An INS/GPS system solves that problem, because it integrates all components outputs and provides the most probable navigation information in any case. When applying it to small UAVs, there is the limitation that only light and small components can be used, at the cost of system accuracy. According to our previous work, an INS/GPS system which consists of MEMS inertial sensors, and a one-frequency GPS receiver with extended KF (EKF) and quaternion algorithms can provide navigation information with errors of several meters in position, several degrees in rolling and pitching, and about ten degrees and in heading. To control small UAVs intelligently, the accuracy of the previous work is not sufficient. Therefore, some improvements are made to the previous work, which are described in section 3..

2.1.2 DSP computing

The existing systems for small UAVs equip micro computers with small calculation power. This is because their guidance and control strategies are simple traditional PID control

with fixed gains. However, in order to control small UAVs more intelligently than human, modern controlling techniques, such as inverse dynamics, $H\infty$, and real-time genetic algorithms (GA) are required. These techniques are represented by matrix operations, and their computational cost is far higher than these micro computers support.

To meet that demand, a floating-point DSP is introduced to the proposed system. A DSP is a processor optimized for simultaneous calculations, such as the product-sum operation used in Fast Fourier Transform (FFT) algorithm, and very suitable for real-time applications like this autopilot system. Although there are other candidates, such as CPUs used in PCs, they are rejected because of large support components and electric power that are difficult to fit into the limited space of a small UAVs body. Moreover, a fixed-point DSP, which performs only fixed-point operations, has the drawback that the range of values must be considered, which is why a floating-point DSP is chosen.

2.2 Prototyping

In order to validate the proposed system, a prototype system is developed. It mainly consists of 6 DOF (degree of freedom) MEMS inertial sensors, a L1-frequency GPS receiver, and a DSP processor. Figures 1,2, and Table 1 show a photograph, the functional diagram, and the main components of the prototype respectively. The size and weight of the prototype are about $50 \times 50 \times 50$mm and under 100g respectively, which is small and light enough for installation into small UAVs. It is functionally divided into four parts: sensor, recorder, calculation, and interface, which will be discussed consecutively.

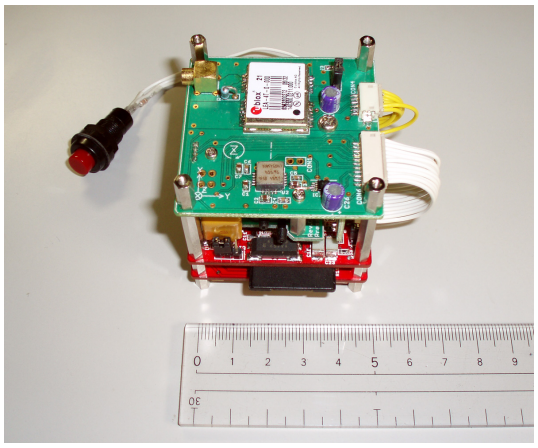

Fig. 1 Prototype (without interface part)

Table. 1 Main components of prototype

Item	Qty	Description
Processor 1 (Main)	1	Texas Instruments TMS320C6713B (200 MHz Floating-Point DSP)
Processor 2 (Sub)	1	Silicon Laboratories C8051F340 (48 MHz 8-bit Micro computer)
Glue logic	1	Xilinx XC3S200 (FPGA, 2M gates)
Acceleromter	1	STMicroelectronics LIS3L02AS4 (3 axes, MEMS)
Gyro	3	Analog Devices ADXRS150 (1 axis, MEMS)
GPS receiver	1	u-blox TIM-4T (L1-frequency, 4 Hz output)

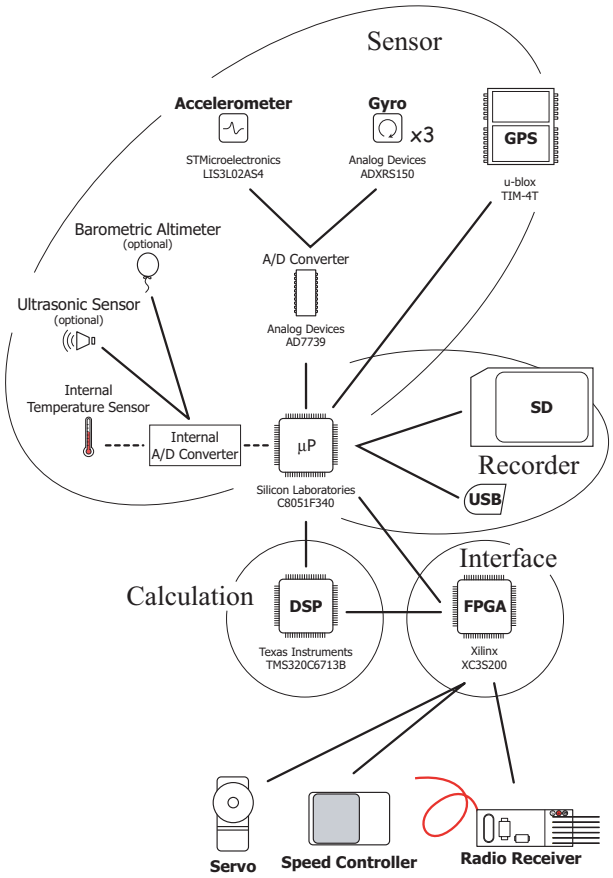

Fig. 2 Functional diagram of prototype

2.2.1 Sensor part

This part includes all sensors whose outputs are inputs of the INS/GPS algorithm. The tri-axes angular speed and tri-axes acceleration outputs which are measured by MEMS inertial sensors, i.e., MEMS gyros, and a MEMS accelerometer respectively, are converted into digital values by a 24-bit Analog / Digital converter (ADC). A GPS receiver measures the current position and velocity, and transmits the data to other parts at 4 Hz. A temperature sensor for thermal correction of sensors is located in the sub-processor. A barometric sensor for measuring relative altitude, and a gauge sensor for measuring relative speed against air are also available.

2.2.2 Recorder part

This part saves and manages the trajectory and command history. A SD card hosted by the sub processor is used to store these data, and has a capacity to log for several hours. A USB interface provides connectivity to a PC and supports to read the data stored in the SD card.

2.2.3 Calculation part

This part performs computational operations of INS/GPS navigation, guidance, and control with the main processor, a floating-point DSP. The calculation performance of the DSP is 1600MIPS / 1200MFLOPS, which is powerful enough for small UAVs to control with modern advanced algorithms.

2.2.4 Interface part

This part manages the connection between this prototype and external devices, such as a wireless communication unit, and servos which actuate control surfaces. This function is provided by a FPGA (Flexible Programming Gate Array), which reconfigures the internal circuit by software corresponding to the connected devices.

3. INS/GPS IMPROVEMENT

In this section, the proposed methods to improve the INS/GPS navigation accuracy are described. This is motivated by the result of our previous study, which shows that the heading error of an INS/GPS system which consist of low grade components, i.e., MEMS inertial sensors and a civil-use GPS receiver, is about ten degrees. This heading error is unacceptable for control of small UAVs, because even in moderate wind the attitude of small UAVs is easily disturbed and large sideslip angles are generated. Therefore, in the proposed autopilot system, two improvements especially for heading accuracy are implemented. The effectiveness of these methods is verified through a real flight test, which is described in the next section.

3.1 Previous Algorithm

Before the methods are described, the algorithm of the previous study is explained shortly. It is divided into two phases of the extended Kalman filtering (EKF), time update and measurement update.

3.1.1 Time Update

This stage is performed as time passes, and the estimated state values $\hat{\underline{x}}$ are updated with

$$\hat{\underline{x}}_{t+1} = \hat{\underline{x}}_t + \int_{\Delta t} f(\hat{\underline{x}}, \hat{\underline{u}}), \tag{1}$$

where $\hat{\underline{u}}$ are the observed inputs, because the relation between the true state values $\underline{x}$ and the true inputs $\underline{u}$ is

$$\frac{d}{dt}\underline{x} \equiv f(\underline{x}, \underline{u}). \tag{2}$$

In the INS/GPS algorithm, $\underline{x}$ is composed of the velocity $\dot{\vec{r}}_e^n$, terrestrial position (i.e., latitude, longitude, and azimuth angle) $\tilde{q}_e^n$, altitude h, and attitude $\tilde{q}_n^b$. $\underline{u}$ corresponds to acceleration $\vec{a}^b$, angular speed $\vec{\omega}_{b/i}^b$ and gravity $\vec{g}^n$. That is

$$\underline{x} \equiv \begin{bmatrix} \dot{\vec{r}}_e^n \\ \tilde{q}_e^n \\ h \\ \tilde{q}_n^b \end{bmatrix}, \quad \underline{u} \equiv \begin{bmatrix} \vec{a}^b \\ \vec{\omega}_{b/i}^b \\ \vec{g}^n \end{bmatrix}. \tag{3}$$

$\hat{\vec{a}}^b$ and $\hat{\vec{\omega}}_{b/i}^b$ are obtained from the accelerometer and the gyros respectively.

Simultaneously, the system covariance update is performed according to

$$P_{t+1} = \Phi P_t \Phi^{\mathrm{T}} + \Gamma_t Q_t \Gamma_t^{\mathrm{T}}, \tag{4}$$

where P and Q are the system error covariance and the input error covariance of the EKF respectively, i.e,

$$P \equiv E\left[\Delta\underline{x}(\Delta\underline{x})^{\mathrm{T}}\right], \quad Q \equiv E\left[\Delta\underline{u}(\Delta\underline{u})^{\mathrm{T}}\right]. \tag{5}$$

The symbol Δ represents the difference value between the estimated value and the true value, and matrices Φ, Γ are derived from Eq. (2).

3.1.2 Measurement Update

The measurement update is performed when the GPS receiver outputs its observed values $\underline{z} \equiv \left[\dot{\vec{r}}_e^n \quad \tilde{q}_e^n \quad h\right]_{\mathrm{GPS}}^{\mathrm{T}}$. The relation between $\underline{x}$ and $\underline{z}$ is called the observation equation:

$$\underline{z} = h(\underline{x}) + \underline{v}, \tag{6}$$

and it is deformed using the notation Δ:

$$\underline{z} - h(\hat{\underline{x}}) = -H_\Delta \Delta\underline{x} + \underline{v}, \tag{7}$$

where H_Δ is defined according to

$$H_\Delta \Delta\underline{x} \equiv h(\hat{\underline{x}}) - h(\underline{x}), \tag{8}$$

and $\underline{v}$ is the error of the observed value $\underline{z}$. Then, $\hat{\underline{x}}$ and P are renewed by the following equations:

$$K_t \equiv P_t H_{\Delta t}^{\mathrm{T}} (H_{\Delta t} P_t H_{\Delta t}^{\mathrm{T}} + R_t)^{-1} \tag{9}$$

$$P_t \leftarrow (I - K_t H_{\Delta t}) P_t \tag{10}$$

$$\Delta\hat{\underline{x}}_t \equiv K_t (z_t - H_{\Delta t}\hat{\underline{x}}) \tag{11}$$

$$\hat{\underline{x}}_t \leftarrow \hat{\underline{x}}_t - \Delta\hat{\underline{x}}_t, \tag{12}$$

where R is the observation error covariance, i.e.,

$$R \equiv E\left[\underline{v}(\underline{v})^{\mathrm{T}}\right]. \tag{13}$$

3.2 Bias Estimation

The first improvement is to estimate the bias drift of inertial sensors. MEMS inertial sensors have low stability of zero outputs, and it is assumed that including its model is effective to reduce the time correlated error. This method modifies Eq. (3) to

$$\underline{x}' = \begin{bmatrix} \underline{x} \\ \vec{a}^b{}_{\mathrm{bias}} \\ \vec{\omega}_{b/i}^b{}_{\mathrm{bias}} \end{bmatrix}, \quad \underline{u}' = \begin{bmatrix} \vec{a}^b + \vec{a}^b{}_{\mathrm{bias}} \\ \vec{\omega}_{b/i}^b + \vec{\omega}_{b/i}^b{}_{\mathrm{bias}} \\ \vec{g}^n \end{bmatrix}, \tag{14}$$

where $\vec{a}^b$ and $\vec{\omega}_{b/i}^b$ are the bias drift, and modeled depending on the first-order Gauss Markov process:

$$\frac{d}{dt}\begin{bmatrix} \vec{a}^b{}_{\mathrm{bias}} \\ \vec{\omega}_{b/i}^b{}_{\mathrm{bias}} \end{bmatrix} = -B\begin{bmatrix} \vec{a}^b{}_{\mathrm{bias}} \\ \vec{\omega}_{b/i}^b{}_{\mathrm{bias}} \end{bmatrix} + \underline{w}, \tag{15}$$

where B is a diagonal matrix and $\underline{w}$ is the white noise with a covariance represented by a matrix S.

Then, Eq. (4) is redefined as

$$P'_{t+1} = \Phi'_t P'_t \Phi'^{\mathrm{T}}_t + \Gamma'_t \begin{bmatrix} Q & 0 \\ 0 & S \end{bmatrix} \Gamma'^{\mathrm{T}}_t, \tag{16}$$

where

$$\Phi' = \begin{bmatrix} \Phi & \Gamma_{\mathrm{sensor}} \\ 0 & -B\Delta t \end{bmatrix}, \quad \Gamma' = \begin{bmatrix} \Gamma & 0 \\ 0 & -I\Delta t \end{bmatrix}, \tag{17}$$

and the observation equation Eq. (7) is also redefined to

$$H_\Delta \leftarrow \begin{bmatrix} H_\Delta & 0 \end{bmatrix}. \tag{18}$$

3.3 Lever Arm Effect

The second improvement utilizes the lever arm effect originating from the difference in the locations where the INS and the GPS antenna are fixed in order to enhance the attitude observability.

The degraded attitude accuracy partly results from the low observability of the attitude and the low accuracy of MEMS gyros. When an INS and a GPS are located at nearly the same position the observation equation Eq. (6) modified according to the previous section is

$$\begin{bmatrix} \dot{\vec{r}}_n^e \\ \tilde{q}_e^n \\ h \end{bmatrix}_{\mathrm{GPS}} = \begin{bmatrix} I & 0 & 0 & 0 & 0 \\ 0 & I & 0 & 0 & 0 \\ 0 & 0 & I & 0 & 0 \end{bmatrix} \begin{bmatrix} \dot{\vec{r}}_n^e \\ \tilde{q}_e^n \\ h \\ \tilde{q}_n^b \\ \underline{b} \end{bmatrix} + \underline{v}, \tag{19}$$

There is no hint related to attitude, because the elements in the forth column of the matrix on the right hand-side are zeros. This drawback is especially influencing the accuracy of the heading, because there is no other support for heading, unlike the roll and pitch, which can be compensated using the gravity vector.

To improve attitude accuracy, augmentation of the observability of attitude is proposed. Suppose that the GPS antenna is fixed at a location different from the INS. In this case, the velocity $\dot{\tilde{r}}_n^e$ and position $\tilde{q}_e^n, h$ obtained by the GPS receiver are also functions of the attitude $\tilde{q}_n^b$, lever arm vector $\vec{l}$, and angular speed $\vec{\omega}_{b/n}$ (see Fig. 3), and the observation equation becomes

$$\begin{bmatrix} \dot{\tilde{r}}_n^e \\ \tilde{q}_e^n \\ h \end{bmatrix}_{\mathrm{GPS}} = \begin{bmatrix} I & 0 & 0 & \not{0} & \not{0} \\ 0 & I & 0 & \not{0} & 0 \\ 0 & 0 & I & \not{0} & 0 \end{bmatrix} \begin{bmatrix} \dot{\tilde{r}}_n^e \\ \tilde{q}_e^n \\ h \\ \tilde{q}_n^b \\ \underline{b} \end{bmatrix} + \underline{v}. \tag{20}$$

where $\not{0}$ indicates a varying non-zero value. This equation shows that the outputs of the GPS receiver include clues for the attitude.

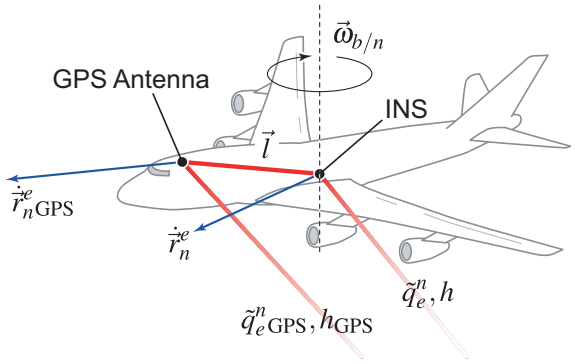

Fig. 3 Lever arm effect

4. FLIGHT TEST

In order to measure the performance of the navigation part of the proposed system and to validate the effectiveness of the proposed method to improve the navigation accuracy, a comparative test with both the original prototype and an ultra-accurate INS/GPS device called GAIA [3] developed by JAXA (Japan Aerospace Exploration Agency) is performed in real flight. This validation test is same as in the previous study. The test result is shown in Tables 2-3, which summarize some statistical values of the difference between GAIA and the prototypes.

Table 3, which applies to the proposed method, indicates better performance than Table 2, whose INS/GPS algorithm is the same as in the previous study. Especially, the improvement in the heading is large, and the history of the sideslip angle against ground-speed shown in Fig. 4 supports this fact.

Table. 2 Prototype navigation accuracy (not improved)

	Mean	Standard deviation	Worst
Horizontal [m]	6.44	2.97	17.0
Altitude [m]	0.85	2.10	6.90
North speed [m/s]	0.00	0.12	1.25
East speed [m/s]	0.00	0.12	−1.13
Down speed [m/s]	−0.08	0.10	−0.67
Rolling [deg]	0.00	0.26	−1.19
Pitching [deg]	−0.67	1.21	−3.90
Heading [deg]	4.17	9.68	23.9

The test result proves that the proposed methods improve the accuracy. Now, the navigation accuracy of the proposed autopilot is sufficient for controlling small UAVs intelligently.

Table. 3 Prototype navigation accuracy (improved)

	Mean	Standard deviation	Worst
Horizontal [m]	5.93	2.75	14.5
Altitude [m]	3.41	1.50	6.78
North speed [m/s]	0.00	0.11	1.03
East speed [m/s]	−0.00	0.10	−1.00
Down speed [m/s]	−0.12	0.08	−0.69
Rolling [deg]	−0.02	0.19	0.82
Pitching [deg]	−0.33	0.35	−1.82
Heading [deg]	−0.69	2.90	7.41

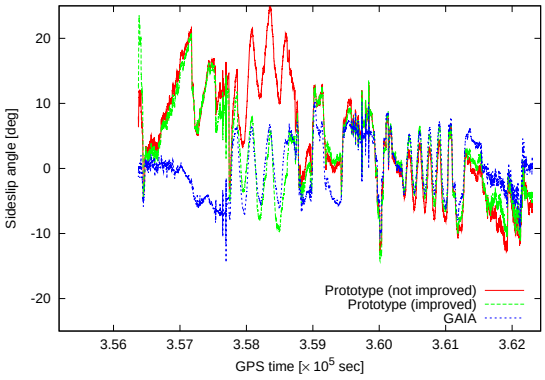

Fig. 4 Sideslip angle history

5. CONCLUSION

A new autopilot system for small UAVs has been proposed. In order to operate small UAVs more intelligently, two novel features, accurate INS/GPS navigation with small MEMS inertial sensors and a civil-use GPS receiver, and large computational capacity derived from a DSP, are incorporated in with the system. A prototype system has been developed, and a performance test of the navigation part of the system has been performed. The result proved that our system provides navigation information accurate enough for controlling small UAVs, and the modifications to the previous study, which are to estimate the bias drift of inertial sensors, and to enhance the attitude observability, are effective. Finally, the authors would also like to thank JAXA for carring out the flight tests using MuPAL-a, and one of suthors M, Naruoka was supported through the 21st Century COE Program, “Mechanical Systems Innovation”, by the Ministry of Education, Culture, Sports, Science and Technology.

REFERENCES

[1] M, Naruoka, T, Tsuchiya, “A Portable and Cost-effective Configuration of Strap-down INS/GPS for General-purpose Use”, *KSAS-JSASS Joint International Symposium on Aerospace Engineering, Busan, Korea*, 2006.

[2] Naruoka, M, and Tsuchiya, T, “High performance navigation system with integration of low precision MEMS INS and general-purpose GPS”, *Transactions of the Japan Society for Aeronautical and Space Sciences, Vol.51, No.171*, 2008. (in press)

[3] Harigae, M, Tomita, H, and Nishizawa, T, “Development of High Precision GPS Aided InertialNavigation”, *Journal of the Japan Society for Aeronautical and Space Sciences, Vol.50, No.585, pp.416-425*, 2002. (in Japanese)